Bacterial Catabolism of a Lignin-derived β–5 Dimer

Naofumi Kamimura, [a],* and Eiji Masai [a]

*[a]Department of Materials Science and Bioengineering, Nagaoka University of Technology,
Nagaoka 940-2188, Japan;
Corresponding author: zkami@vos.nagaokaut.ac.jp

Abstract

The β–5 linkage is an intermolecular linkage in lignin. *Sphingobium* sp. strain SYK-6 can assimilate various lignin-derived dimers, including a β–5 dimer, dehydrodiconiferyl alcohol. In SYK-6, the hydroxyl group at Cγ of the B-ring side chain of dehydrodiconiferyl alcohol is oxidized to generate the γ-carboxylic compound, DCA-C. Then, the hydroxyl group at Cγ of the A-ring side chain of DCA-C is oxidized to the carboxyl group to generate the dicarboxylic compound, DCA-CC. The carboxylic group at Cγ of the A-ring side chain of DCA-CC is decarboxylated, and the accompanying spontaneous ether cleavage of the coumaran ring produces a stilbene-type compound, DCA-S. The conversions of DCA-C and DCA-CC are catalyzed by enantiospecific oxidases (PhcC and PhcD) and enantiospecific decarboxylases (PhcF and PhcG), respectively. DCA-S is subjected to cleavage of the interphenyl double bond by lignostilbene α,β-dioxygenase to generate 5-formylferulate and vanillin. Among the eight lignostilbene α,β-dioxygenase genes, vanillate-induced *lsdD* plays a critical role in cleaving DCA-S. The formyl group of 5-formylferulate is oxidized, and the resultant carboxylic group is subsequently decarboxylated to produce ferulate. Finally, ferulate and vanillin are further catabolized via a previously characterized pathway.

Keywords: Enantiospecific enzymes; Lignostilbene α,β-dioxygenase; β–5 linkage; Phenylcoumaran; Sphingobium sp. SYK-6

Lignin, a phenylpropanoid polymer, is a major plant cell wall component and the most abundant aromatic polymer on earth. The microbial degradation of lignin is a critical part of the global carbon cycle, and its catalytic ability is beneficial for lignocellulosic biomass utilization. In lignin, phenylpropane units derived from monolignols are connected via C–C and C–*O*–C linkages [1,2]. In addition to the predominant β–*O*–4 (β-aryl ether) linkage, lignin has β–5 (phenylcoumaran), 5–5 (biphenyl), β–β (resinol), and β–1 (spirodienone) linkages. Microbial degradation of lignin proceeds in two main stages: "depolymerization of native lignin by white-rot fungi," and "mineralization of the resultant aromatic compounds by bacteria." Therefore, elucidating the bacterial catabolism of lignin-derived aromatic compounds is crucial for understanding the final stage of lignin biodegradation in nature.

The β–5 linkage connects two monolignols via C–C and C–*O*–C linkages (Fig. 1) and accounts for 9–12% and 3–11% of the total intermonomer linkages in softwood and hardwood lignin, respectively [3]. Dehydrodiconiferyl alcohol (DCA), a typical β–5 dimer, is one of the major dilignols generated in the initial stages of lignin polymerization [4,5]. Studies of microbial β–5 dimer degradation has mainly been conducted by Japanese researchers. The first report was a 1978 study by Katayama and Fukuzumi [6]. DCA was used as a β–5 dimer, and its degradation pathway by *Pseudomonas putida* FK-2, isolated from an effluent treatment pond in a kraft pulp mill, was partly proposed. After this report, the fungal degradation pathway of DCA was determined in *Fusarium solani* and *Phanerochaete chrysosporium* by Takayoshi Higuchi's research group [7-9]. In 1988, an outline of the bacterial DCA catabolic pathway in *Sphingomonas paucimobilis* TMY1009 was proposed by Habu *et al* [10]. Subsequently, enzymes, thought to be involved in one reaction step of DCA catabolism, were identified and characterized by Kamoda *et al* [11-15]. In recent years, our research group has uncovered a more detailed DCA catabolic pathway, through the analysis of DCA catabolism genes in *Sphingobium* sp. SYK-6 [16-19]. This review
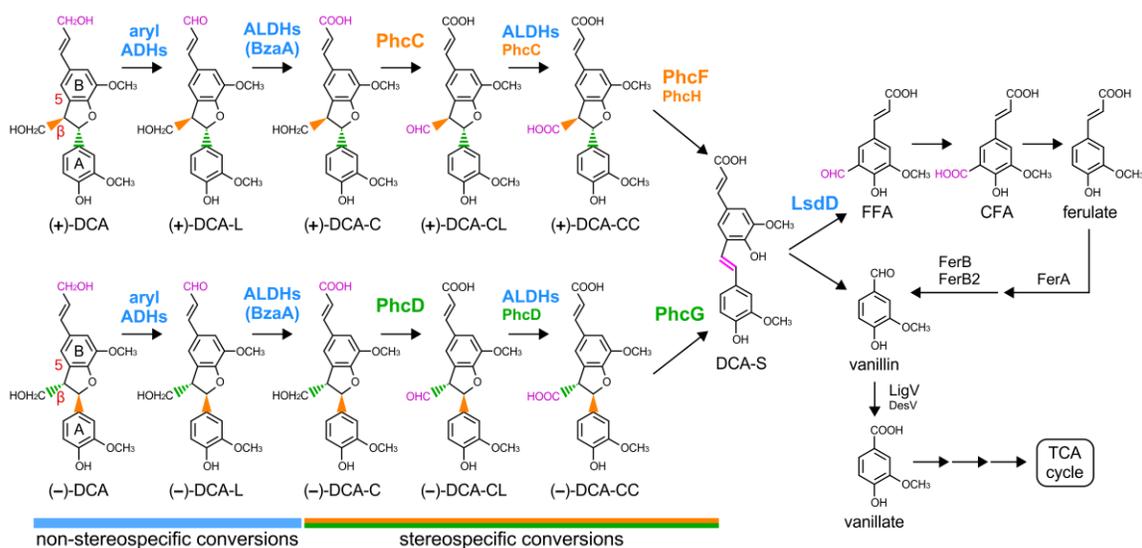
Fig. 1. Catabolic pathway of a β-5 dimer, DCA in *Sphingobium* sp. SYK-6.
Enzymes: ADH, alcohol dehydrogenase; ALDH, aldehyde dehydrogenase; PhcC, (+)-DCA-C oxidase; PhcD, (−)-DCA-C oxidase; PhcF and PhcH, (+)-DCA-CC decarboxylases; PhcG, (−)-DCA-CC decarboxylase; LsdD, lignostilbene α,β-dioxygenase; FerA, feruloyl-coenzyme A (CoA) synthetase; FerB and FerB2, feruloyl-CoA hydratase/lyases; LigV, vanillin dehydrogenase; DesV, syringaldehyde dehydrogenase. Compounds: DCA, dehydrodiconiferyl alcohol; DCA-L, 3-(2-(4-hydroxy-3-methoxyphenyl)-3-(hydroxymethyl)-7-methoxy-2,3-dihydrobenzofuran-5-yl)acrylaldehyde; DCA-C, 3-(2-(4-hydroxy-3-methoxyphenyl)-3-(hydroxymethyl)-7-methoxy-2,3-dihydrobenzofuran-5-yl)acrylate; DCA-CL, 3-(3-formyl-2-(4-hydroxy-3-methoxyphenyl)-7-methoxy-2,3-dihydrobenzofuran-5-yl)acrylate; DCA-CC, 5-(2-carboxyvinyl)-2-(4-hydroxy-3-methoxyphenyl)-7-methoxy-2,3-dihydrobenzofuran-3-carboxylate; DCA-S, 3-(4-hydroxy-3-(4-hydroxy-3-methoxystyryl)-5-methoxyphenyl)acrylate; FFA, 5-formylferulate; CFA, 5-carboxyferulate.

describes advances in our knowledge of bacterial DCA catabolism, which consists of a group of enzymes, including stereospecific oxidases, stereospecific decarboxylases, and side-chain cleavage oxygenases.

Sphingobium sp. SYK-6 is the best-characterized bacterium for catabolism of lignin-derived aromatic compounds [20,21]. This strain catabolizes various lignin-derived dimers, including β-aryl ether, biphenyl, diarylpropane, and phenylcoumaran, as well as monomers, such as ferulate, vanillin, vanillate, syringaldehyde, and syringate. The study of DCA catabolism in SYK-6 was carried out much by the doctoral thesis of our alumnus Kenji Takahashi, who started with pathway determination in 2014 (Fig. 1) [16]. In SYK-6, DCA catabolism is initiated by oxidation of the hydroxyl group at Cγ of the B-ring side chain to produce 3-(2-(4-hydroxy-3-methoxyphenyl)-3-(hydroxymethyl)-7-methoxy-2,3-dihydrobenzofuran-5-yl)acrylate (DCA-C) via the aldehyde derivative, 3-(2-(4-hydroxy-3-methoxyphenyl)-3-(hydroxymethyl)-7-methoxy-2,3-dihydrobenzofuran-5-yl)acrylaldehyde (DCA-L). Thereafter, the hydroxyl group at Cγ of the A-ring side chain of DCA-C is oxidized to generate 5-(2-carboxyvinyl)-2-(4-hydroxy-3-methoxyphenyl)-7-methoxy-2,3-dihydrobenzofuran-3-carboxylate (DCA-CC) via the aldehyde derivative 3-(3-formyl-2-(4-hydroxy-3-methoxyphenyl)-7-methoxy-2,3-dihydrobenzofuran-5-yl)acrylate (DCA-CL). The carboxyl group at Cγ of the A-ring side chain of DCA-CC is further decarboxylated to form a stilbene-type compound, 3-(4-hydroxy-3-(4-hydroxy-3-methoxystyryl)-5-methoxyphenyl)acrylate (DCA-S). The interphenyl Cα–Cβ double bond is then cleaved to generate vanillin and 5-formylferulate from the A- and B-ring portions, respectively. Finally, the formyl group of 5-formylferulate is oxidized, and the resultant carboxyl group is decarboxylated to produce ferulate. This catabolic pathway is fundamentally similar to that suggested in TMY1009. Furthermore, another phenylcoumaran catabolic pathway through 3-methoxy-4-hydroxyphenylglyoxal has been proposed in *Rhodococcus jostii* RHA1 [22].

SYK-6 has at least three and four genes encoding quinohemoprotein alcohol dehydrogenases and aryl alcohol dehydrogenases, respectively, which oxidize DCA to DCA-L [16]. Generally, quinohemoprotein alcohol dehydrogenase uses pyrroloquinoline quinone as the prosthetic group [23], whereas aryl alcohol dehydrogenase requires $NAD(P)^+$ as a coenzyme for the reaction [24]. Since SYK-6 cell extracts require NAD^+ as a coenzyme to oxidize DCA, aryl alcohol dehydrogenases probably play a major role in DCA oxidation. In the next DCA-L oxidation step, aldehyde dehydrogenases (ALDHs) appeared to be involved. SYK-6 has 23 ALDH genes, and multiple ALDH genes are often involved in the oxidation of aromatic aldehydes, such as vanillin, syringaldehyde, vanilloyl acetaldehyde, and syringoyl acetaldehyde [25-27]. Of the 23 ALDH genes, 14 gene products were able to oxidize DCA-L [16]. BzaA showed the highest DCA-L oxidation activity, and disruption of *bzaA* in SYK-6 reduced DCA-L conversion ability. Therefore, while multiple ALDHs are involved in DCA-L oxidation in SYK-6, *bzaA* seems to play a major role in this step.

DCA contains two chiral carbons at the Cα and Cβ positions of the A-ring side chain, and the relative configurations of both carbons are *trans*. Hirai *et al*. determined the absolute configurations of DCA to be (+)-(2*S*,3*R*)-DCA and (−)-(2*R*,3*S*)-DCA (Fig. 1) [28]. In SYK-6, DCA and DCA-L are presumed to be oxidized non-stereospecifically, because the aryl alcohol dehydrogenases and ALDHs, described above, exhibit no stereospecificity (unpublished results). In contrast, DCA-C oxidation and DCA-CC decarboxylation are stereospecific [17,18]. Glucose-methanol-choline (GMC) oxidoreductase family enzymes, PhcC and PhcD, oxidize the hydroxyl group at Cγ of the A-ring side chain of (+)-DCA-C and (−)-DCA-C with strict enantiospecificity, respectively [17]. *phcC* and *phcD* were identified based on the cofactor requirements and transcription induction profiles. Mutant analyses demonstrated that *phcC* and *phcD* are essential for the oxidation of the corresponding DCA-C isomer. Both PhcC and PhcD are localized to the membrane and cytoplasm and can oxidize DCA-C using ubiquinone derivatives, such as CoQ_0 and CoQ_1 as electron acceptors. Therefore, electrons removed from DCA-C by oxidation appeared to be transferred to cytochrome *c* via ubiquinone in vivo. Interestingly, a GMC oxidoreductase family enzyme (HpvZ) is also involved in the oxidation of β-hydroxypropiovanillone, a phenylpropane-type intermediate in β-aryl ether catabolism [27]. Thus, the GMC oxidoreductase family enzymes play important roles in the oxidation of the side chain hydroxyl group at Cγ of some lignin-derived compounds in SYK-6. PhcC and PhcD can oxidize DCA-CL in addition to DCA-C (Fig. 1); however, NAD^+-dependent ALDHs have been suggested to play a significant role in the oxidation of DCA-CL to DCA-CC [17].

PhcF and PhcG catalyze the decarboxylation of the carboxyl group at Cγ of the A-ring side chain of (+)-DCA-CC and (−)-DCA-CC, respectively, to generate DCA-S with strict enantiospecificity (Fig. 1). PhcF and PhcG showed 32% amino acid sequence identity with each other, but there was no significant similarity with known enzymes. Both proteins have a DUF3237 domain with unknown functions. In March 2022, 2546 proteins with the DUF3237 domain are registered (https://pfam.xfam.org/family/PF11578); however, the proteins whose functions have been demonstrated are only PhcF and PhcG, in addition to PhnH, which catalyzes enantioselective hydroalkoxylation of an intermediate of the herqueinone biosynthetic pathway in *Penicillium herquei* [29]. Structural analysis of PhnH showed that this protein forms a β-barrel fold and contains a large central cavity that serves as the putative substrate-binding pocket [30]. Structural comparison of PhnH with some DUF3237 members suggested that these proteins exhibit a similar overall fold. PhcF and PhcG are homotrimers, and their K_m values for DCA-CC were determined to be 84 μM and 103 μM, and V_{max} were 307 μmol·min⁻¹·mg⁻¹ and 137 μmol·min⁻¹·mg⁻¹, respectively [18]. In addition to PhcF and PhcG, a nuclear transport factor 2 (NTF2)-like superfamily domain protein, PhcH, exhibits (+)-DCA-CC specific decarboxylation activity (Fig. 1). These genes are localized in tandem and consist of a *phcH-phcG-phcF* operon (unpublished results). Mutant analyses of *phcF*, *phcG*, and *phcH* demonstrated that both *phcF* and *phcG* play major roles in DCA-CC decarboxylation, with a minor contribution from *phcH*. In contrast, the triple mutant of *phcF*, *phcG*, and *phcH* retained a small amount of activity. SYK-6 has six and three homologs of *phcF*/*phcG* and *phcH*, respectively. Among the nine homologs, two *phcF*/*phcG* homologs (SLG_07290 and SLG_28660) and one *phcH* homolog (SLG_30010) exhibited faint activity. These multiple homologs or a different type of decarboxylase may play minor roles in DCA-CC decarboxylation.

An achiral stilbenoid, DCA-S, is formed by the decarboxylation of DCA-CC and cleavage of the α–O–4 linkage in the coumaran ring caused by electron transfer from the carboxylate anion associated with decarboxylation. DCA-S is subjected to cleavage of the interphenyl double bond, by lignostilbene α,β-dioxygenase (LSD), to generate 5-formylferulate and vanillin (Fig. 1). Among the eight LSD genes in SYK-6, the gene products of *lsdA*, *lsdC*, *lsdD*, and *lsdG* exhibited DCA-S conversion activity [19]. The DCA-S conversion activity of SYK-6 was induced by vanillate, and the transcription of *lsdA*, *lsdD*, and *lsdG* was induced in the presence of vanillate. Mutant analyses demonstrated that *lsdD* plays a critical role in the conversion of DCA-S during DCA catabolism. In SYK-6, a MarR-type repressor, DesR, which responds to vanillate and syringate, regulates the vanillate and gallate catabolism genes, as well as its own gene [31]. *lsdD* is adjacent upstream of *desR* in the opposite transcription direction. Moreover, the location of the DesR-binding site (IR-R) for *desR* regulation is immediately upstream of the start codon of *lsdD*. These facts suggest that the binding of DesR to IR-R represses transcription of not only *desR,* but also *lsdD*. Recently, Eltis and coworkers revealed the enzymatic and structural features of LsdD of SYK-6 (LSD4 in the nomenclature used by their group) and LsdA of TMY1009 [32,33]. The overall fold of LsdD is a seven-blade β-propeller fold with a cap-like feature on one face formed by extended loops. This structure is common to LsdA of TMY1009 and carotenoid cleavage dioxygenases [32,34]. A catalytic iron(II) ion is bounded to the bipyramidal coordination sphere, distorted by four conserved histidines (His-167, 218, 284, and 476 of LsdD) and a water molecule. The key catalytic residues of LsdD, Phe-59, Tyr-101, and Lys-134 were also conserved. LSDs exhibit a broad substrate range for stilbenoids [19,32], and all SYK-6 LSDs catalyze the cleavage of 1,2-bis(4-hydroxy-3-methoxyphenyl)-1,3-propanediol (HMPPD-S) [19]. HMPPD-S is an intermediate metabolite of a β–1 dimer in TMY1009 [35] and *Novosphingobium aromaticivorans* DSM 12444 [36], and similarly in SYK-6. Among SYK-6 LSDs, LsdH showed the highest oxidizing activity toward HMPPD-S, and its gene transcription level was also the highest during the growth of SYK-6 with vanillate [19]. *lsdH* is likely involved in converting HMPPD-S during β–1 catabolism.

The DCA catabolic pathway has been clarified, and the enzyme genes involved in the steps from DCA oxidation to DCA-S cleavage have been elucidated. Additionally, our research group recently demonstrated the 5-formylferulate catabolic system at the 65th lignin symposium [37]. So, are we close to a complete understanding of the β–5-type dimer catabolic system? It seems there is still quite a long way to go. Firstly, substrate uptake and transcriptional regulation systems are poorly understood. Secondly, we recently discovered that the DCA catabolic pathway is altered in induced and non-induced cells (unpublished results). The pathway presented in this review was determined using cells grown under non-inducing conditions. However, under DCA-inducing conditions, oxidation of the A-ring side chain of DCA, and cleavage of the interphenyl double bond, appear to occur before oxidation of the B-ring side chain of DCA. This observation suggests that the DCA catabolic pathway is altered during culture. Thirdly, DCA, a guaiacyl-type β–5 dimer, is generally used for catabolic studies; however, syringyl- and *p*-hydroxyphenyl-type β–5 dimers also exist [38-40]. In addition, it is not known how the DCA catabolic system of SYK-6 works for the actual β–5 structure-derived compounds produced by lignin biodegradation in nature. Further progress in a more detailed and comprehensive elucidation of the catabolism of β–5 dimers is expected, considering the points mentioned above.

REFERENCES

1) Ralph, J. *et al.*, Lignin structure and its engineering, *Curr Opin Biotechnol*, **56**, 240-249 (2019).

2) Vanholme, R. *et al.*, Lignin biosynthesis and structure, *Plant Physiol*, **153**, 895-905 (2010).

3) Zakzeski, J. *et al.*, The catalytic valorization of lignin for the production of renewable chemicals, *Chem Rev*, **110**, 3552-3599 (2010).

4) Tanahashi, M. *et al.*, Dehydrogenative polymerization of 3,5-disubstituted *p*-coumaryl alcohols, *Wood Res*, **61**, 44-53 (1976).

5) Davin, L. B. *et al.*, Stereoselective bimolecular phenoxy radical coupling by an auxiliary (dirigent) protein without an active center, *Science*, **275**, 362-366 (1997).

6) Katayama, Y., Fukuzumi, T., Bacterial degradation of dimers structurally related to lignin. II. Initial intermediate products from dehydrodiconiferyl alcohol by *Pseudomonas putida*, *Mokuzai Gakkaishi*, **24**, 643-649 (1978).

7) Nakatsubo, F. *et al.*, Metabolism of a phenylcoumaran substructure lignin model compound in ligninolytic cultures of *Phanerochaete chrysosporium*, *Arch Microbiol*, **128**, 416-420 (1981).

8) Ohta, M. *et al.*, Microbial degradation of dehydrodiconiferyl alcohol, a lignin substructure model, *Arch Microbiol*, **121**, 23-28 (1979).

9) Umezawa, T. *et al.*, Lignin degradation by *Phanerochaete chrysosporium*: Metabolism of a phenolic phenylcoumaran substructure model compound, *Arch Microbiol*, **131**, 124-128 (1982).

10) Habu, N. *et al.*, Metabolic pathway of dehydrodiconiferyl alcohol by *Pseudomonas* sp. TMY1009, *Mokuzai Gakkaishi*, **34**, 1026-1034 (1988).

11) Kamoda, S. *et al.*, Purification and some properties of lignostilbene-α,β-dioxygenase isozyme IV from *Pseudomonas paucimobilis* TMY1009, *Biosci Biotechnol Biochem*, **61**, 1575-1576 (1997).

12) Kamoda, S., Samejima, M., Cloning of a lignostilbene-α,β-dioxygenase gene from *Pseudomonas paucimobilis* TMY1009, *Agric Biol Chem*, **55**, 1411-1412 (1991).

13) Kamoda, S., Saburi, Y., Structural and enzymatical comparison of lignostilbene-α,β-dioxygenase isozymes, I, II, and III, from *Pseudomonas paucimobilis* TMY1009, *Biosci Biotechnol Biochem*, **57**, 931-934 (1993).

14) Kamoda, S., Saburi, Y., Cloning, expression, and sequence analysis of a lignostilbene-α,β-dioxygenase gene from *Pseudomonas paucimobilis* TMY1009, *Biosci Biotechnol Biochem*, **57**, 926-930 (1993).

15) Kamoda, S. *et al.*, Purification and some properties of lignostilbene-α,β-dioxygenase responsible for the Cα-Cβ cleavage of a diarylpropane type lignin model compound from *Pseudomonas* sp. TMY1009, *Agric Biol Chem*, **53**, 2757-2761 (1989).

16) Takahashi, K. *et al.*, Characterization of the catabolic pathway for a phenylcoumaran-type lignin-derived biaryl in *Sphingobium* sp. strain SYK-6, *Biodegradation*, **25**, 735-745 (2014).

17) Takahashi, K. *et al.*, Membrane-associated glucose-methanol-choline oxidoreductase family enzymes PhcC and PhcD are essential for enantioselective catabolism of dehydrodiconiferyl alcohol, *Appl Environ Microbiol*, **81**, 8022-8036 (2015).

18) Takahashi, K. *et al.*, Two novel decarboxylase genes play a key role in the stereospecific catabolism of dehydrodiconiferyl alcohol in *Sphingobium* sp. strain SYK-6, *Environ Microbiol*, **20**, 1739-1750 (2018).

19) Kamimura, N. *et al.*, LsdD has a critical role in the dehydrodiconiferyl alcohol catabolism among eight lignostilbene α,β-dioxygenase isozymes in *Sphingobium* sp. strain SYK-6, *Int Biodeterior Biodegradation*, **159**, 105208 (2021).

20) Kamimura, N. *et al.*, Bacterial catabolism of lignin-derived aromatics: New findings in a recent decade: Update on bacterial lignin catabolism, *Environ Microbiol Rep*, **9**, 679-705 (2017).

21) Masai, E. *et al.*, Genetic and biochemical investigations on bacterial catabolic pathways for lignin-derived aromatic compounds, *Biosci Biotechnol Biochem*, **71**, 1-15 (2007).

22) Wei, Z. *et al.*, Characterization of thiamine diphosphate-dependent 4-hydroxybenzoylformate decarboxylase enzymes from *Rhodococcus jostii* RHA1 and *Pseudomonas fluorescens* Pf-5 involved in degradation of aryl C_2 lignin degradation fragments, *Biochemistry*, **58**, 5281-5293 (2019).

23) Toyama, H. *et al.*, Quinohemoprotein alcohol dehydrogenases: structure, function, and physiology, *Arch Biochem Biophys*, **428**, 10-21 (2004).

24) Uthoff, S., Steinbüchel, A., Purification and characterization of an NAD+-dependent XylB-like aryl alcohol dehydrogenase identified in *Acinetobacter baylyi* ADP1, *Appl Environ Microbiol*, **78**, 8743-8752 (2012).

25) Masai, E. *et al.*, Characterization of *ligV* essential for catabolism of vanillin by *Sphingomonas paucimobilis* SYK-6, *Biosci Biotechnol Biochem*, **71**, 2487-2492 (2007).

26) Kamimura, N. *et al.*, A bacterial aromatic aldehyde dehydrogenase critical for the efficient catabolism of syringaldehyde, *Sci Rep*, **7**, 44422 (2017).

27) Higuchi, Y. *et al.*, Bacterial catabolism of β-hydroxypropiovanillone and β-hydroxypropiosyringone produced in the reductive cleavage of arylglycerol-β-aryl ether in lignin, *Appl Environ Microbiol*, **84** (2018).

28) Hirai, N. *et al.*, Absolute configuration of dehydrodiconiferyl alcohol, *Biosci Biotechnol Biochem*, **58**, 1679-1684 (1994).

29) Gao, S. S. *et al.*, Enzyme-catalyzed intramolecular enantioselective hydroalkoxylation, *J Am Chem Soc*, **139**, 3639-3642 (2017).

30) Feng, Y. *et al.*, Crystal structure and proposed mechanism of an enantioselective hydroalkoxylation enzyme from *Penicillium herquei*, *Biochem Biophys Res Commun*, **516**, 801-805 (2019).

31) Araki, T. *et al.*, Regulation of vanillate and syringate catabolism by a MarR-type transcriptional regulator DesR in *Sphingobium* sp. SYK-6, *Sci Rep*, **9**, 18036 (2019).

32) Kuatsjah, E. *et al.*, Identification of functionally important residues and structural features in a bacterial lignostilbene dioxygenase, *J Biol Chem*, **294**, 12911-12920 (2019).

33) Kuatsjah, E. *et al.*, Structural and functional analysis of lignostilbene dioxygenases from *Sphingobium* sp. SYK-6, *J Biol Chem*, **296**, 100758 (2021).

34) Sui, X. *et al.*, Structural basis of carotenoid cleavage: from bacteria to mammals, *Arch Biochem Biophys*, **539**, 203-213 (2013).

35) Habu, N. *et al.*, Metabolism of a diarylpropane type lignin model compound by *Pseudmonas* sp. TMY1009, *Mokuzai Gakkaishi*, **35**, 348-355 (1989).

36) Presley, G. N. *et al.*, Pathway discovery and engineering for cleavage of a β-1 lignin-derived biaryl compound, *Metab Eng*, **66**, 328-329 (2021).

37) Kawazoe, M. *et al.*, Identification and characterization of the 5-formylferulate catabolism genes in *Sphingobium* sp. SYK-6, *The 65th lignin symposium*, pp. 49-50 (2020).

38) Kuroda, K., Nakagawa-Izumi, A., Tetramethylammonium hydroxide thermochemolysis of guaiacyl-syringyl and guaiacyl dehydrogenation polymers, *Org Geochem*, **36**, 53-61 (2005).

39) Rencoret, J. *et al.*, Structural characterization of milled wood lignins from different eucalypt species, *Holzforschung*, **62**, 514-526 (2008).

40) Wei, X. *et al.*, Deciphering the linkage type and structural characteristics of the *p*-hydroxyphenyl unit in *Pinus massoniana Lamb* compressed wood lignin, *Int J Biol Macromol*, **208**, 772-781 (2022).